Heliyon 11 (2025) e41223

Contents lists available at ScienceDirect

Heliyon

journal homepage: www.cell.com/heliyon

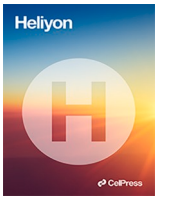

Research article

Experimental investigations of colloid-associated metal mobility in mine-impacted wetland sediment

Colleen O. Harper *, Richard T. Amos

Department of Earth Sciences, Carleton University, 1125 Colonel By Dr, Ottawa, ON, K1S 5B6, Canada

ARTICLE INFO

Keywords:
Colloid-facilitated transport
Zinc
Metal attenuation
Contamination
Legacy mine-waste

ABSTRACT

Metal mining operations can release toxic metals to surrounding environments where site-specific conditions control the movement of contaminants. Colloid-facilitated transport, the transport of contaminants with small, mobile particles, has been recognized as a potential contaminant transport vector in groundwater, but it remains unclear under what conditions it is important and whether neutral, metal-rich mine drainage from legacy mining impacts this transport vector. This work presents a set of laboratory column experiments that study the effect of colloids on metal mobility in saturated, wetland sediment that has been receiving neutral mine drainage for nearly a century, using mixed and single metal input solutions at neutral pH. Results indicate that colloid-facilitated transport is only important when small (<0.01 μm) colloids, most likely formed from organic matter, are present. Larger particles were found to be generally immobile, so could aid in the immobilization of metal contaminants. These findings imply that colloid-facilitated transport is an important transport vector in mine-impacted wetland sediment and should be considered when remediating mine sites.

1. Introduction

Contamination from metal mining operations is a major environmental challenge with toxic metals released from waste-rock piles significantly degrading water quality [1,2]. Waste impoundments, both waste-rock and tailings, can pose serious risks to areas in immediate proximity to mines, but contaminant transport increases the area impacted. Contaminant transport is highly site-specific, with solution chemistry, physical characteristics of the porous media, and flow patterns all impacting how contaminants migrate.

Ordinarily, transport is conceptualized as a two-phase system consisting of an immobile solid phase and an aqueous phase; however, small mobile particles, colloids, can participate in metal transport creating a three-phase transport scenario where a carrier phase is added [3]. Colloids have similar characteristics to solids, so can readily interact with metal ions that have an affinity to the solid phase [4]. If these particles are present and act to enhance metal mobility, the apparent solubility of metals can be higher and contamination can be observed at distances that would not be expected under a two-phase system [5–7]. Colloid-facilitated transport has been a research focus over the last several decades in an attempt to determine how much impact colloids have on metal mobility and whether colloids are always contaminant transport vectors [8,9]. A large base of research has indicated that metal contamination can be impacted by colloids, allowing them to be carried farther than anticipated [8]. Colloid-facilitated transport can be impacted by changing concentrations of colloids [10], the presence of organic molecules such humic acid [7,11], and a complex solution

* Corresponding author.
E-mail address: colleenharper@cmail.carleton.ca (C.O. Harper).

https://doi.org/10.1016/j.heliyon.2024.e41223
Received 10 December 2024; Accepted 12 December 2024
Available online 13 December 2024

composition [12].

Colloids are generally defined as particles less than 10 μm in size [13] that form when particles are released from the solid matrix or as solids precipitate from solution [14]. A wide range of materials form colloids, including geologic materials such as clay particles or other mineral fragments, organic matter including humic and other organic substances, and microorganisms including living or dead bacteria cells [9,15]. The composition and source of colloids can be controlled by the (bio)geochemistry of an area [8]. Colloids are ubiquitous in both groundwater and surface water [16], so are expected to be readily available to participate in colloid-facilitated contaminant transport. Many researchers have found evidence for colloid-facilitated transport at both laboratory [4,7,10, 12, 17–19] and field scales [20–24], but it remains unclear whether colloids participate in metal transport in all scenarios [10].

While the aqueous transport of contaminants has been extensively studied in and around mine-waste impoundments, research generally focuses on recently placed waste-rock piles [2,25–27] or legacy mine sites that have been partially remediated or had mitigation efforts implemented [28,29]. To our knowledge fewer studies have focused on legacy mine sites that have not undergone any remediation. Because both physical and chemical properties (e.g., the pH, ionic strength, Eh, and conductivity) of the subsurface may impact colloid mobility [8], it is possible that long-term contamination, which could expose the subsurface to high quantities of metal contaminants, has the potential to alter whether colloid-facilitated transport is an important process at legacy mine sites.

The objective of the current experimental, laboratory study was to examine whether colloid-facilitated transport is important in saturated wetland sediment that has received continuous metal-rich drainage from an abandoned, uncontrolled waste-rock pile located at the Ore Chimney Mine property near Kaladar, Ontario, replicating, as much as possible, existing field conditions. Zinc was the primary target metal in these experiments due to high quantities of sphalerite in the waste rock which has been shown to be highly weathered [30], leading to elevated Zn concentrations in the wetlands adjacent to the waste rock [31]. Field-collected sediment and natural, sediment-derived colloids were used to allow for a representation of long-term contamination impacts. The effects of solution composition, flow rate and colloid suspension characteristics were investigated.

2. Methods

2.1. Sediment source and description

Sediment used in this study was collected from a wetland adjacent to a waste-rock pile at the Ore Chimney Mine property. The property is located in the area of Kaladar and Barrie townships, approximately 100 km northwest of Kingston, ON [32,33]. Underground operations at the mine occurred between 1909 and 1932 [33] and targeted a gold-bearing quartz-carbonate vein system [34, 35]. It is not clear when the waste-rock pile was first constructed, but it was approximately its current size in the 1930s (based on aerial images taken in 1934 [36]). The waste rock contains high concentrations of sulfide minerals including galena, sphalerite, pyrite, and others [37], as well as carbonate minerals such as calcite [30]. High degrees of mineral weathering were identified by Hicks [30], with sphalerite being the most weathered. Investigations of the wetland groundwater and sediment identified elevated concentrations of Zn and other metal contaminants near the waste-rock pile, with limited transport beyond approximately 30 m from the edge of the waste rock [31].

Sediment was collected in late October 2020 using a steel auger and stored in plastic bags. Sediment was kept frozen at approximately −20 °C and thawed for use in April 2022. Sediment used for this experiment consisted of a fine-grained organic sediment collected approximately 1 m below the sediment/water interface, in the same area as sediment characterized by Harper et al. [31]; it was determined that the sediment contained an average of 79 % organic matter (maximum 90 %) in this area of the Ore Chimney wetland. All sediment collected at the site was saturated due to standing water in the wetland.

2.2. Column physical parameters and packing

Experiments consisted of a set of two, 30.5 cm long by 3 cm diameter columns constructed of polyvinyl chloride (PVC) bodies and caps, with sample ports and inflow/outflow lines constructed of 0.6 cm semi-rigid high-density polyethylene (HDPE) tubing and stainless-steel Swagelok® fittings. Five sample ports were constructed at 5 cm intervals along the length; HDPE tubes extended roughly 2.5 cm into the column with approximately 20 small holes punched along this length. Glass wool was used to loosely pack the sample tube and prevent sediment from entering the sample port. Teflon tape was used on all threaded connections. A piece of Nitex nylon mesh with 100 μm pores was placed in each end cap to prevent sediment from entering inflow and outflow lines.

Columns were packed with a volumetric mixture of 15 % Ore Chimney wetland sediment and 85 % quartz sand (classified grain size 30/40 mesh). This mixture was used to reduce the overall sorption capacity of the column packing so that experiments could be run in a reasonable time frame. The ratio was chosen based on batch experiments that indicated high adsorption capacity of the organic-rich sediment (Supplemental Materials 1), and previous analysis of the wetland sediment that showed high metal loads including up to approximately 9000 mg/kg Zn, 2700 mg/kg Pb, and 275 mg/kg Cd [31]. Although adding quartz sand modified the natural character of the sediment, the quartz was determined to have low sorption capacity for Zn (Figure S1.2); this configuration was used to provide faster breakthrough of metals and colloids through the column. A layer of approximately 1 cm of sand was added to the bottom of the column and the sediment/sand mixture was added, scoop-wise with gentle tapping on the sides of the column to remove air pockets and homogenize layers. All packing was saturated with deionized water prior to addition to the columns. Columns were allowed to rest, undisturbed, for 24 h to allow settling to occur, and additional sediment/sand mixture was added if settling had lowered the level of the sediment in the column. Porosity of the column packing (15 % wetland sediment and 85 % sand) was estimated prior to addition to columns by drying then saturating a sample to determine the volume of void space (Supplemental Materials 2). Porosity ranged from

30 % to 40 %.

2.3. Column operation – flow, experimental phases, and input solutions

Flow to the columns was controlled with a peristaltic pump (Masterflex® L/S® precision variable-speed console drive with Masterflex® L/S® standard pump head for precision tubing and L/S® 13 Puri-Flex™ precision pump tubing). Flow rates were continuously monitored, and pump tubing was replaced as needed if it became clogged or flow rate in the column dropped. Flow in the columns was from bottom to top to ensure continuous saturation, and the column was kept vertical.

The experiment was run in three consecutive phases; Phase 1 had a target flow rate of 0.15 mL/min, (range of 0.12 mL/min to 0.17 mL/min), corresponding to a linear flux of approximately 100 m/year. In Phase 2, the flow rate was doubled to approximately 0.3 mL/min (range of 0.32 mL/min to 0.33 mL/min), corresponding to a linear flux of approximately 200 m/year. In Phase 3, the higher flow rate was maintained (range of 0.22–0.33 mL/min), but the colloid composition of the input solution was changed (discussed below). During Phase 1, approximately 2 pore volumes were replaced each day and in Phases 2 and 3, approximately 4 pore volumes were replaced each day. Samples were collected every three days regardless of flow rate. Phase 1 lasted 90 days, Phase 2 lasted 18 days, and Phase 3 lasted 30 days. Phase lengths were selected by actively monitoring metal and colloid concentrations and starting the next phase once all parameters were relatively stable, or when it was clear that the previous change did not result in a significant change in measured parameters. Variation in flow rate was due to pump tube clogging and wear of the pump tubing.

Input solutions to the columns consisted of metal solutions that contained colloids extracted from the Ore Chimney sediment. Colloid extraction was conducted using methods similar to those used by Roy and Dzombak [38] and Jiang et al. [17]. Sediment was thoroughly mixed with deionized water using a wrist action shaker and allowed to settle for 24 h so larger particles settled out. Since colloids do not easily settle from solution [39], colloids remained in suspension and were syphoned off, being careful not to disturb settled sediment. For Phases 1 and 2, this suspension was centrifuged at 3000 rpm for 60 min to concentrate colloids, and the supernatant (any liquid above the visible colloid mass) was removed and discarded. The concentrated colloids that remained were rinsed with NaCl (to remove exchangeable cations) and then deionized water to minimize the concentration of solutes released from the Ore Chimney sediment and decrease their addition to input solution concentrations. The concentrated colloids were dried so a known mass of colloids could be added to the solution. For Phases 1 and 2, there was the potential for small colloids to be lost if they remained in the supernatant after centrifuging.

In Phase 3, to ensure as complete a colloid suspension as possible and prevent the loss of the smallest particles, the centrifuging and drying steps were removed, and the colloid suspension was used without additional preparation to make the input solution. For many elements, this led to concentrations of metals and other solutes in the input solution that were greater than the target metal concentration (i.e., what was added from the stock solutions) because they were not removed by rinsing during colloid preparation (Table 1). These higher concentrations were considered the new input concentrations to allow for determinations of whether the higher concentrations impacted the results. For all experimental phases, magnetic stir plates were used to continuously mix input solutions and ensure homogeneous distribution of colloids.

Metal solutions were prepared with reagent grade solutions or salts of each metal diluted to the appropriate concentration with deionized water or the Phase 3 colloid suspension. Column 1 used a $ZnCl_2$ solution with no other metals added to the solution to allow individual metal responses to be investigated (Table 1). To replicate effluent conditions from the Ore Chimney waste rock, investigate

Table 1
Input solution parameters for each column including the metal ions and their total aqueous concentration, and the concentration of colloids. Metal concentrations determined by ICP-MS. Colloid concentration in Phase 3 was measured in Nephelometric Turbidity Units (NTU) and converted to concentration (mg/L) (see Supplemental Materials 3 for details).

Constituent	Column 1			Column 2		
	Concentration (ppb)			Concentration (ppb)		
	Input solution (Target)	Input solution using extracted colloids (Measured) Phases 1 and 2	Input solution using colloid suspension (Measured) Phase 3	Input solution (Target)	Input solution using extracted colloids (Measured) Phases 1 and 2	Input solution using colloid suspension (Measured) Phase 3
Al	0	0	180	0	0	180
Ca	0	830	35160	6000	7020	41350
Cd	0	0	0	500	0	0
Cu	0	0	20	100	0	20
Fe	0	0	30	0	0	30
K	0	20	2380	5000	6030	8380
Mg	0	40	5320	5000	5090	10380
Mn	0	0	80	100	90	170
Na	5750	6370	7050	10750	9980	10650
Ni	0	0	0	100	70	70
Pb	0	0	0	50	0	0
Zn	15000	8920	9740	15000	11770	12590
Colloids (mg/L)	75	75	194	75	75	194

metal mobility in an un-remediated wetland sediment and to allow for the investigation of competitive adsorption with multiple metals present, Column 2 used a mixed metal solution containing metals that were found in the Ore Chimney waste-rock porewater [30] and wetland groundwater [31]. Concentrations of each metal were chosen based on previous research findings from the site to align with environmentally relevant concentrations (Table 1). The pH of each solution was adjusted to pH 7 with a 30 % NaOH solution.

2.4. Sampling and analysis

Samples of approximately 25–30 mL were collected at the sample ports by closing the effluent port and opening the sample port. Earlier experiments (unpublished) indicated that dissolved oxygen (DO) is consumed in columns using this sediment, so samples were collected in sealed, $N_{2(g)}$ purged flasks and kept in a low oxygen environment (less than 5 % O_2) during processing to ensure stable redox conditions. Initial sampling started with only the port closest to the inlet and sampling of the other ports began after approximately 40 pore volumes. When more than one port was sampled, the column was allowed to run for at least 30 min between sampling to re-establish flow in the column. Samples were collected at the first sample port (5 cm along column length), the middle sample port (15 cm along column length), and the end sample port (25 cm along column length).

All sample preparation and testing was conducted in an oxygen depleted, $N_{2(g)}$ environment with less than 5 % $O_{2(g)}$. Prior to additional sample preparation, all samples were tested for pH with an Oakton Ion 700 pH bench meter with a Cole-Parmer pH probe (accuracy of $\pm$0.01 pH units) and turbidity with an Apera Instruments TN420 turbidity meter to allow for the determination of colloid concentration (see Supplemental Materials 3). Samples were filtered with a Sterlitech polycarbonate stirred-cell filter and polycarbonate filter membranes with pore sizes of 10 μm, 1 μm, 0.1 μm, and 0.01 μm. Filtering was completed sequentially with the filtrate from the previous filter pore size being filtered at the next largest pore size to prevent filter blinding from larger particles. The entire 30 mL sample was filtered and approximately 6 mL of sample was saved after each filter size. Anything not removed by the 0.01 μm filter was considered part of the dissolved phase, since the 0.01 μm filter size was the lower limit of the filtration equipment available. All samples were saved in 15 ml plastic centrifuge tubes, acidified to pH of ~2 with approximately 50 μL of 70 % trace-metal grade nitric acid, and refrigerated at 4 °C until metal concentrations could be analyzed. Aqueous samples were tested for metal concentrations with inductively coupled plasma mass spectrometry (ICP-MS). The analysis of samples with ICP-MS allows for the determination of total metal concentration (dissolved plus colloidal) since colloids are ionized during analysis. Detection limits for each element in ICP-MS analysis were calculated as three times the standard deviation of a series of blank samples tested after instrument calibration through all runs (used for Na, Mg, Al, K, Ca, Fe, and Zn), or as the concentration of the lowest calibration standard (0.1 ppb) if the calculated detection limit was lower than this value (used for Mn, Ni, Cu, Cd, and Pb) [40]. Internal standards contained 10 % methanol to improve consistency in the internal standard recovery and reduce matrix effects during analysis that resulted from the high organic carbon content present in the samples.

Scanning electron microscopy (SEM) coupled with energy dispersive X-ray spectroscopy (EDS) was used to image colloids on filter membranes. Samples were coated with gold to increase conductivity and imaged with both back scatter electron and secondary electron imaging. While EDS provided general elemental composition, because the samples were not smooth or uniform, it was not possible to use this technique to determine exact percentages of the composition.

2.5. Column dismantling and porewater extraction/analysis

At the end of the experiment, column packing was removed with a plastic spoon, separating upper and lower portions of the columns. Samples were stored in plastic bags and refrigerated at 4 °C.

Porewater was extracted from the column packing through centrifugation. Centrifuge tubes (50 mL) were altered to allow for the separation of water and sediment. A centrifuge tube was shortened to the 30 mL mark and a small hole was drilled in the tip. A small amount of glass wool was placed at the tip and the tube was filled with roughly 25 mL of the column packing. Another centrifuge tube was shortened to the 20 mL mark and placed under the sediment packed tube to collect the water. Samples were centrifuged at 3000 rpm for 5 min. Two 25 mL portions of sediment were centrifuged for both the upper and lower sections of the column, resulting in approximately 20 mL of water which was filtered using the same processes as for all other water samples, acidified and refrigerated. Water samples that were collected through centrifugation of column packing from the sediment in the lower part of the column had sediment loads that were too high to allow for filtering, so these samples did not go through processing or testing. After filtration and acidification, particles settled from filtered porewater samples that had been collected from the upper part of the column, so analysis was only conducted on the liquid above the settled particles to ensure particles would not clog ICP-MS components.

2.6. Data processing and analysis

For quality control, duplicate samples were collected throughout the experiment and the results of these duplicates were averaged to provide a single value for that sample. Colloid concentrations in samples were determined by converting the measured turbidity values from NTU to mg/L using calibration curves created from both colloid suspension methods (Supplemental Materials 2). Turbidity results were excluded from analysis if column flow problems (e.g., clogged tubing or stopcocks not being opened) caused pressure to build in the column leading to a sudden release of sediment when flow was re-established.

Sample and porewater data were analyzed to determine if there were large portions of metals associated with colloids and any specific particle size fraction. The percent of total concentration associated with any size fraction was determined for filtrate samples. Size classes were assigned (Table 2) and concentrations in each class were determined by subtracting the results from the next smallest

filter. The percent of total metal concentration was determined with Equation (1). For water testing results, the data from the three size classes (A, B, and C) were grouped to give two categories, colloidal (>0.01 μm) and dissolved (<0.01 μm).

$$\%\ of\ total = \frac{Concentration\ in\ Size\ Class}{Total\ Concentration} \times 100 \quad (1)$$

Where the total concentration is considered the concentration of the 10 μm filtered sample.

For analysis of associations between major cations/metals and colloids, outliers were removed. Outliers were considered any concentration that was greater than three standard deviations above the mean of the three non-suspect filtrate concentrations of that sample. Fewer than 0.2 % of any column's results were identified as outliers and removed.

3. Results

3.1. Colloid characteristics

Colloid morphology varied between size classes (Fig. 1), but colloids were similar between columns. The largest sized colloids had highly irregular morphology (with colloids generally being composed of aggregates of smaller particles) and generally resembled the morphology of humic acid observed by other researchers [e.g., 41]. Colloids below 10 μm in size and above 1 μm, were also generally irregular, but some platy particles were observed. Below 1 μm in size, particles were more regular in shape with a largely circular or oblong shape. Due to limitations of SEM, particles present on the 0.01 μm filters could not be distinguished.

Compositional analysis (EDS) of particles on filter membranes revealed high quantities of carbon and oxygen, but it was not possible to determine exact elemental ratios because of the surface morphology of the particles. A few particles had measurable concentrations of Fe, Al, Ca, S, Si, and Mg, but were still primarily composed of C and O. Additional information available in Supplemental Materials 4.

3.2. pH and colloid concentration

Throughout the experiment the pH in both columns remained approximately circum-neutral (defined as pH between 6 and 8 [42]), but did show a moderately acidic pH, particularly in Phase 1 (minimum pH of 5.07) (Fig. 2). In both Columns 1 and 2, the pH was consistent between sampling ports (Fig. 2). The pH varied sample to sample, with the most variability observed near the beginning of the experiment, but pH remained between 5.0 and 6.9.

The colloid concentrations were generally low throughout the experiment but had extreme, single-sample spikes at several points. In Column 1 (Fig. 3A), colloid concentrations were high (179 mg/L) in the first sample from the first port and decreased over the next four samples, reaching a minimum of approximately 10 mg/L. Colloid concentrations were stable at this minimum at the first port with some minor variations throughout the remainder of Phase 1 and all of Phase 2. At the middle port and the end port, colloid concentrations in Column 1 were initially higher than those observed at the first port, and generally decreased to the minimum (with two spikes at 74 pore volumes and 150 pore volumes) throughout the remainder of Phase 1 and all of Phase 2. In Phase 3, colloid concentrations increased substantially at the first port of Column 1 reaching and exceeding the concentration observed in the first sample (maximum of 207 mg/L). The colloid concentrations in the middle and end ports also increased during Phase 3, but not to the same degree as was observed at the first port.

In Column 2 (Fig. 3B), the colloid concentration trend was the same as that observed in Column 1, with the exception of the initial decrease in colloid concentration in the first port. With random concentration spikes at some ports, concentrations were low throughout Phase 1 and 2 (approximately 5 mg/L). As with Column 1, colloid concentrations increased throughout Phase 3, reaching the maximum concentration of 246 mg/L at the first port at 348 pore volumes.

3.3. Major cations– Na, Mg, K, and Ca

In Column 1 (Zn only input solution), low total major cation concentrations were the result of element release from the Ore Chimney wetland sediment in the column packing. The elements Mg, K, and Ca were not included in the input for Column 1; however, Na was present in the input solution from pH adjustment with NaOH. In Column 2 (mixed metal input solution), higher total concentrations of major cations resulted from the presence of these elements in high concentrations in the input solution. In Phase 3 the change in colloid extraction procedure meant that the major cations present in the contaminated sediment remained in solution, rather than being removed during colloid extraction processes, resulting in higher element concentrations in the input solution. For Phase 3,

Table 2
Colloid size class definitions for water analysis.

Size Class	Definition
Class A	Between 1 and 10 μm
Class B	Between 0.1 and 1 μm
Class C	Between 0.01 and 0.1 μm
Class D	Below 0.01 μm (dissolved)

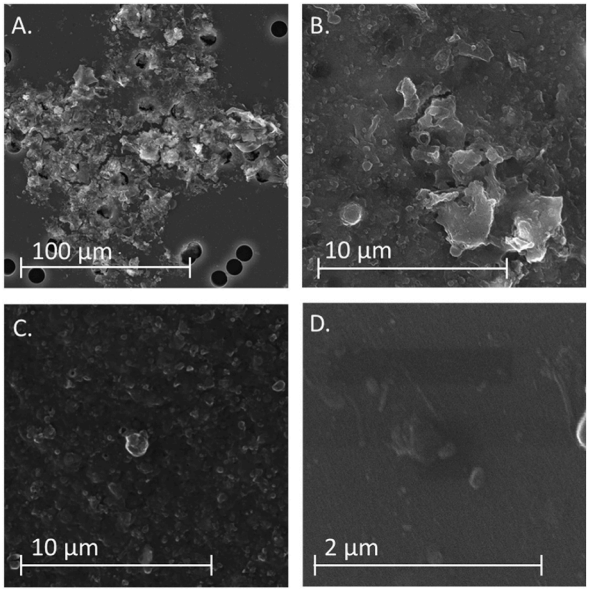

Fig. 1. Representative images of colloids on **A.** 10 µm pore size filter, **B.** 1 µm pore size filter, **C.** 0.1 µm pore size filter, and **D.** 0.01 µm pore size filter. Note the different scale on the different images.

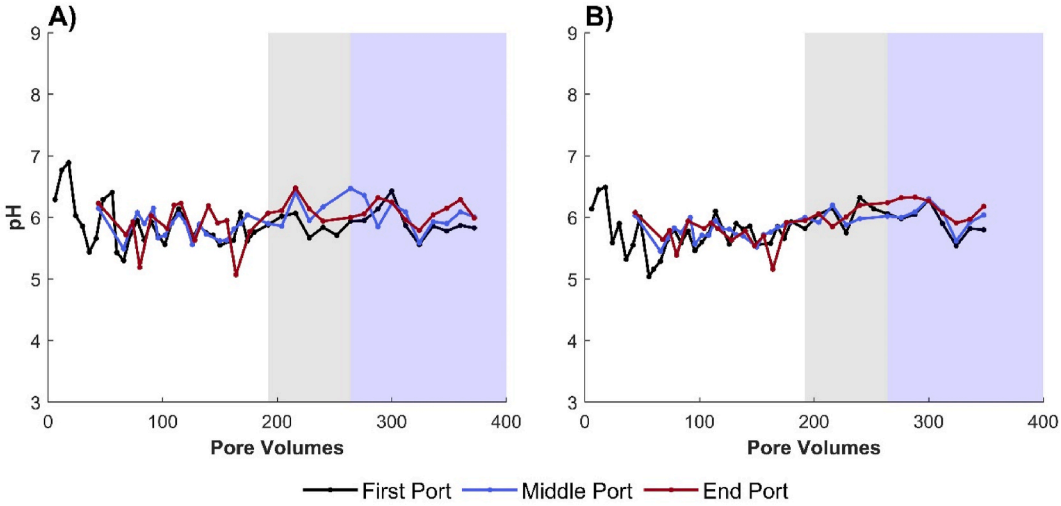

Fig. 2. pH variability of samples (accuracy of ±0.01 pH units) collected from the first, middle, and end ports in **A)** Column 1 and **B)** Column 2. Line colour indicates sample port. Unshaded region indicates Phase 1, grey shaded region indicates Phase 2, and blue shaded region indicates Phase 3.

testing of the uncentrifuged colloid suspension (filtered at 0.45 µm) indicated that an additional 5000 ppb of Mg, 2000 ppb of K, and 34000 ppb Ca were present, increasing the Phase 3 input concentrations to 10000 ppb Mg, 7000 ppb K and 40000 ppb Ca.

Throughout the experiment, total major cation concentrations in samples reflect the input concentrations regardless of column, phase, or sample port (Fig. 4). In Column 1, Na concentrations were generally stable throughout the experiment but showed random concentration spikes (Fig. 4A). It is not clear what caused these concentration spikes, but spikes occurred at the end port (farther along the flow path) near the same pore volume at which a spike was not observed in earlier sample ports; this may have been an artifact of sampling procedure. Calcium was released from the column packing for the first approximately 50 pore volumes; concentrations decreased slightly and stabilized with approximately a 25 pore volume separation between sample ports, indicating that Ca release was progressing through the column (Fig. 4G and H).

Very little association between major cations and colloids was observed in Column 1 (Table 3) or Column 2 (Table 4). Generally, an average of less than 5 % of the total Na, Mg, or Ca concentration was found in association with the colloid sized particles, regardless of experimental phase. The remainder of the total concentration was found in the dissolved (<0.01 µm) phase. Calcium had a few individual samples that had strong associations with colloids (e.g., one sample in Phase 1 of Column 1 where 60.2 % of the total

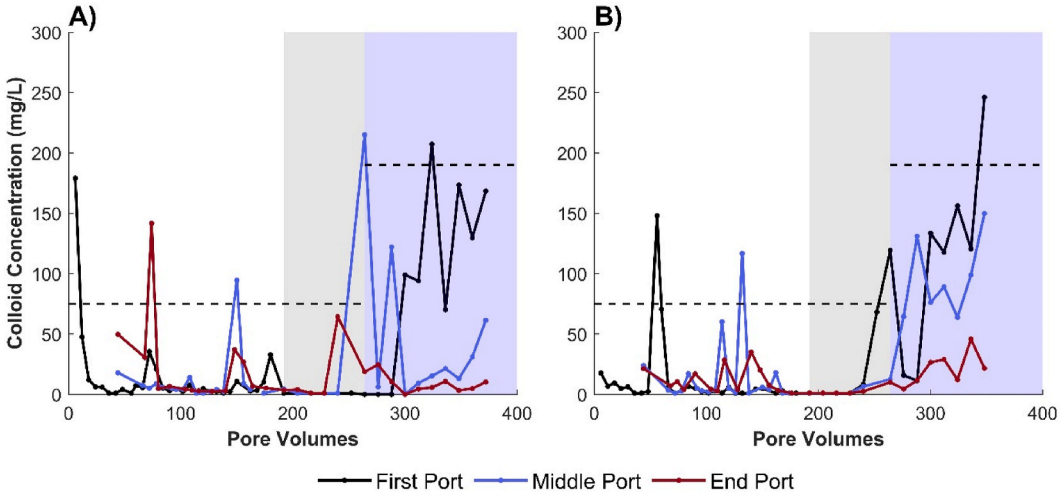

Fig. 3. Colloid concentration of samples collected from the first, middle, and end sample ports in **A)** Column 1 and **B)** Column 2. Line colour indicates sample port. Unshaded region indicates Phase 1, grey shaded region indicates Phase 2 and blue shaded region indicates Phase 3. Black dashed line indicates input solution colloid concentration in each phase.

concentration was associated with colloids), although the average association in each phase (Tables 3 and 4) remained small. Potassium was eliminated from analysis in Column 1 since concentrations were low (close to the detection limit) or below the detection limit, and low levels of contamination were observed, with consistently increasing K concentrations in more filtered samples. Potassium was included in the analysis for Column 2 (Table 4) since concentrations of K in this column were less impacted by contamination and the variability was lower.

3.4. Metals – Al, Fe, Cu, Mn, Ni, Cu, Pb, Cd, and Zn

In Column 1, Zn was the only metal included in the input solution, so any other metal observed in the samples was released from the column packing. To first identify concentration trends more clearly, trends are visualized and discussed based on the 0.01 μm filtered samples only, as these represented the dissolved phase metals; subsequent discussion will include colloidal association.

Aluminum, Fe and Cu had similar dissolved (<0.01 μm) concentration trends in Columns 1 and 2 (Fig. 5A–F). Concentrations of these elements were high in the first sample with the highest concentration found in Column 1. In both columns, concentrations of these metals decreased substantially by the second and third samples and were stable at their concentration minimum throughout the remainder of Phase 1 and the entirety of Phase 2. Aluminum, Fe, and Cu concentrations spiked in both columns at the beginning of Phase 3, particularly in the first port. Concentrations continued to increase, stabilizing by 300 pore volumes. Concentrations began to increase at the middle and end ports at approximately 300 pore volumes.

Dissolved Mn concentrations were stable throughout Phases 1 and 2 with very low concentrations in Column 1 (Fig. 5G) and concentrations of approximately 50 ppb in Column 2 (Fig. 5H). In both columns, Mn concentrations were approximately the same at all three ports. Manganese concentrations began to gradually increase at the beginning of Phase 3; a maximum Mn concentration of approximately 150 ppb was reached in Column 1 and a maximum Mn concentration of approximately 300 ppb was achieved in Column 2, slightly higher than the input concentration. Approximately 80 ppb Mn was found in uncentrifuged colloid suspension, so the Mn input concentration increased in Phase 3.

Dissolved concentrations of both Pb (Fig. 6A and B) and Cd (Fig. 6C and D) were low throughout the duration of the experiment but showed modest increases in both columns throughout Phase 3. Lead concentrations dropped below the detection limit in both columns during Phases 1 and 2 but reached the input concentration in Phase 3 in Column 2. Despite the modest increase in concentration observed in Phase 3, Cd concentrations did not approach the input concentration. Nearly identical trends for Cd were observed between the two columns despite the input concentrations being drastically different.

Dissolved Zn concentrations at the first port in Column 1 increased steadily for the first 50 pore volumes and then stabilized at approximately 5000 ppb (Fig. 6E). The concentration of Zn at all ports spiked at the beginning of Phase 3, then decreased to concentrations close to the input concentration (15000 ppb), but variation was observed. Zinc concentration in the first port spiked to just above the input concentration, while the concentration increased to over 20,000 ppb in the second and third ports. Following the decrease in phase three, the concentration continued to be variable. In Column 2, Zn was more mobile than in Column 1 with higher concentrations throughout the first two phases of the experiment, stabilizing at a concentration of 10,000 ppb (Fig. 6F). Zinc concentrations in Column 2 spiked to close to 20,000 ppb at the beginning of Phase 3 but decreased slightly and stabilized at the input concentration of 15,000 ppb for the remainder of the experiment.

The percent of total metal concentration associated with colloids showed variation. Because approximately one third of samples had Pb concentrations below the detection limit and other samples saw increasing concentrations in increasingly filtered samples, Pb

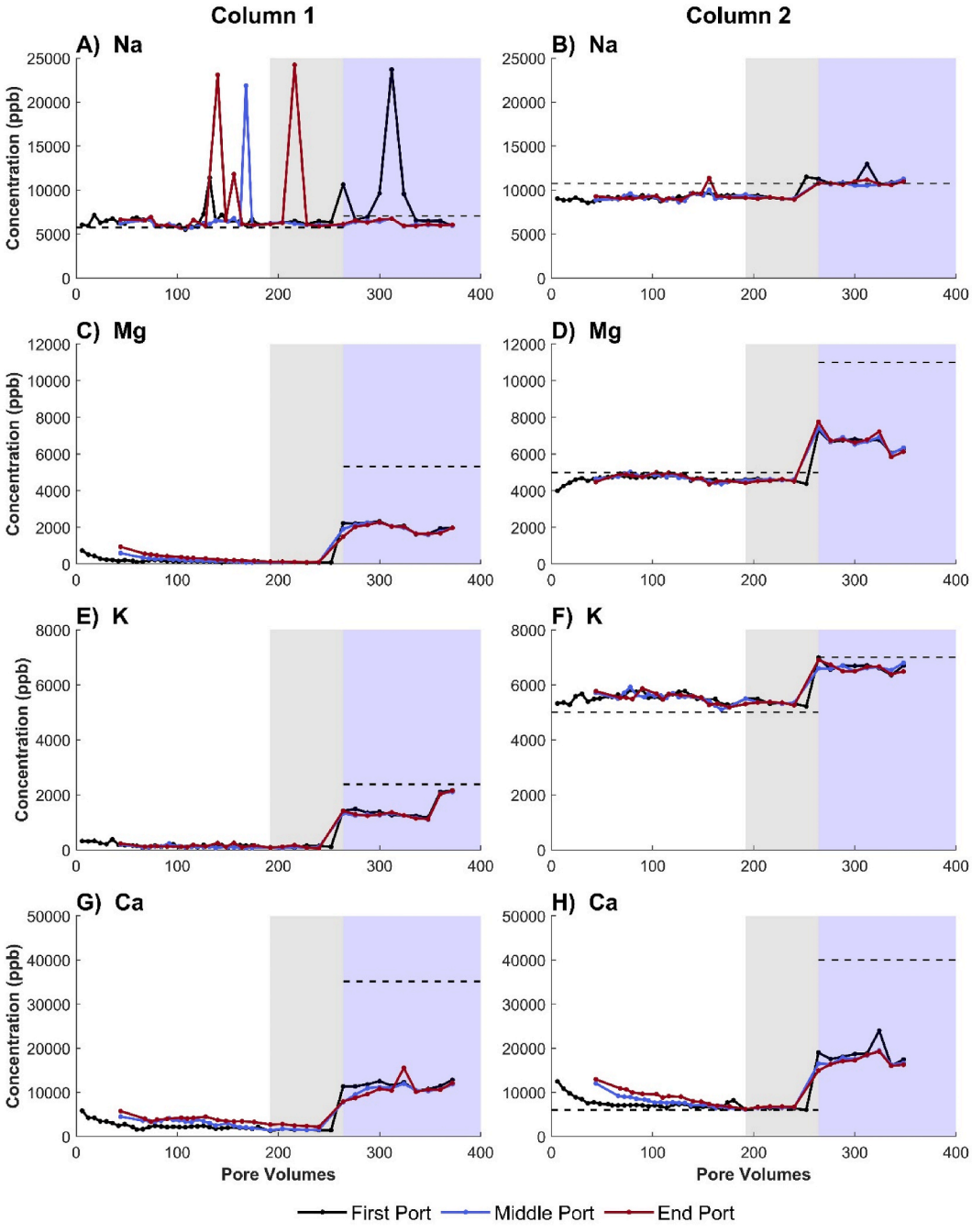

Fig. 4. Dissolved concentrations (<0.01 μm) of major cations in samples collected from Columns 1 and 2 including Na (**A** and **B**), Mg (**C** and **D**), K (**E** and **F**), and Ca (**G** and **H**). Unshaded region indicates Phase 1, grey shaded region indicates Phase 2, and blue shaded region indicates Phase 3. Line colours indicate sampling port. Black dashed line indicates input solution concentration. Note different scale for different elements.

was excluded from analysis of colloid associations in both columns. Associations between Fe and colloids were not calculated for Phase 2 in either column because concentrations in water samples were very low (i.e., <3 ppb) and low levels of contamination during filtering had a substantial impact on results.

The degree of differentiation between filter sizes was variable between metals, columns and experimental phases (Tables 5 and 6, and Supplemental Materials 5). In general, Mn, Zn, and Cd had low association with colloids with less than 20 % of the total metal concentration associated with colloids between 0.01 and 10 μm. Aluminum, Fe and Cu had high percentages of total metal concentration associated with colloids in both columns; Al had between approximately 25 and 65 % associated with colloids, Fe had generally between 20 and 45 % associated with colloids in Phase 3, and Cu had generally between 10 and 55 % associated with colloids (Tables 5

Table 3
Average percent of total major cation concentration associated with colloidal sizes (between 0.01 μm and 10 μm) and in the dissolved phase (<0.01 μm) for Column 1. Percentages that were found to be negative values or greater than 100 %, which resulted from testing variation, sample heterogeneity and/or contamination of samples that went through more filter steps, were replaced with 0 or 100 (%), respectively. Averages were only calculated if greater than 3 samples were above detection limits.

Colloid Class →		First Port		Middle Port		End port	
		Colloidal	Dissolved	Colloidal	Dissolved	Colloidal	Dissolved
Metal	Phase	>0.01 μm (%)	<0.01 μm (%)	>0.01 μm (%)	>0.01 μm (%)	<0.01 μm (%)	<0.01 μm (%)
Na	**1**	2.2	97.8	2.3	97.7	2.0	98.0
	2	0	100	0	100	0.2	99.8
	3	0.3	99.7	0.2	99.8	0.2	99.8
Mg	**1**	0	100	0	100	0	100
	2	0	100	0	100	0	100
	3	0	100	0	100	0	100
Ca	**1**	0	100	0	100	0.1	99.9
	2	0	100	0	100	0	100
	3	0	100	0	100	0	100

Table 4
Average percent of total major cation concentration associated with colloidal sizes (between 0.01 μm and 10 μm) and in the dissolved phase (<0.01 μm) for Column 2. Percentages that were found to be negative values or greater than 100 %, which resulted from testing variation, sample heterogeneity and/or contamination of samples that went through more filter steps, were replaced with 0 or 100 (%), respectively. Averages were only calculated if greater than 3 samples were above detection limits.

Colloid Class →		First Port		Middle Port		End port	
		Colloidal	Dissolved	Colloidal	Dissolved	Colloidal	Dissolved
Metal	Phase	>0.01 μm (%)	<0.01 μm (%)	>0.01 μm (%)	<0.01 μm (%)	>0.01 μm (%)	<0.01 μm (%)
Na	**1**	1.7	98.3	0.9	99.1	1.2	98.8
	2	0	100	0	100	0	100
	3	1.4	98.6	0.6	99.4	0.7	99.3
Mg	**1**	3.5	96.5	2.7	97.3	3.1	96.9
	2	0.7	99.3	0.3	99.7	1.5	98.5
	3	3.1	96.9	1.0	99.0	0.8	99.2
K	**1**	0	100	0	100	0	100
	2	0	100	0	100	0	100
	3	2.5	97.5	1.1	98.9	1.3	98.7
Ca	**1**	1.7	98.3	0.9	99.1	1.2	98.8
	2	0	100	0	100	0	100
	3	1.4	98.6	0.6	99.4	0.7	99.3

and 6). The percent of total metal concentration associated with colloids was similar in Columns 1 and 2, and minor variation was observed between experimental phases and sample ports.

3.5. Extracted porewater results

High percentages of trace elements were associated with colloid sized particles in porewater samples extracted from the column packing at the end of the experiments (Table 7). These colloids, however, were not mobile and remained in the column porewater rather than exiting the column with the effluent. These particles were only mobilized during centrifuging of the column packing samples.

In filtered porewater samples from both Column 1 and Column 2, the majority of the major cations Na, Mg, and K were found primarily in the dissolved phase (between 80 % and 99 %) (Table 7). Calcium was also primarily associated with the dissolved phase (66.3 % in Column 1 and 58.0 % in Column 2), however a significant amount, approximately 25 %, was associated with a single colloidal size fraction, either Class B in Column 1 or Class A in Column 2 (Supplemental Materials 5).

Extracted porewater data showed variable results for metal concentrations, but all metals had some percentage of their total concentration associated with a colloid size class. In both columns, the majority of Al was associated with a colloid size fraction with 68 % associated with Class B in Column 1, and 57 % in Class A and 34 % in Class B in Column 2 (Supplemental Materials 5). A maximum of 16 % of Al was found in the dissolved phase. Iron had similar results to aluminum. In Column 1, 62 % of Fe was associated with Class B colloids while in Column 2, 56 % was associated with Class A and 33 % was associated with Class B colloids (Supplemental Materials 5). Results for Cu, Zn, Cd, and Pb were similar with higher percentages associated with Class A particles in Column 2 than was found in Column 1. The highest percentage of total metal concentration associated with colloids was found for Al, Fe, Cu and Pb in Column 2 with approximately 10 % in the dissolved phase (Table 7 and Supplemental Materials 5).

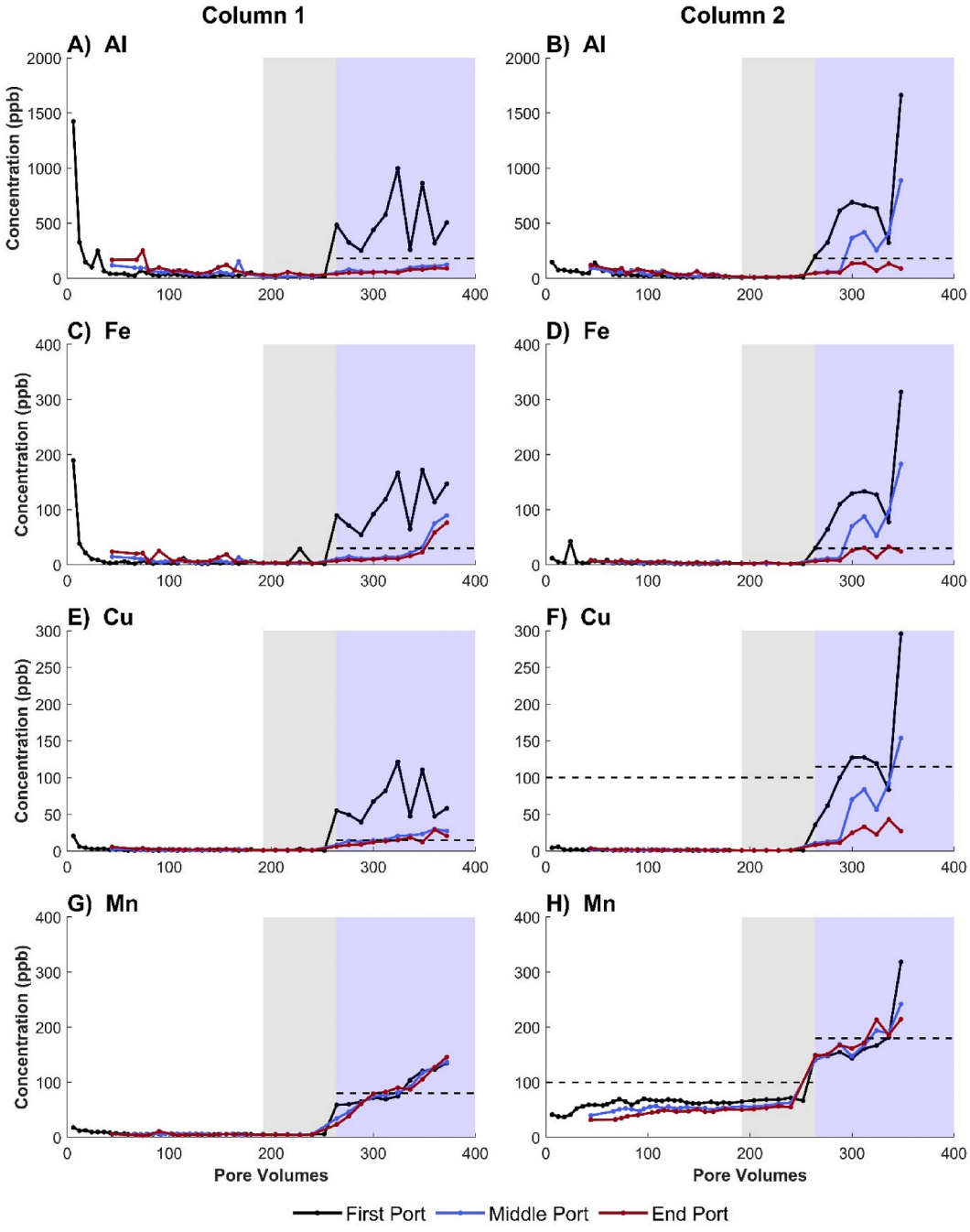

Fig. 5. Dissolved (<0.01 μm) metal concentrations for samples collected from sampling ports (indicated by line colours) for Al (**A** and **B**), Fe (**C** and **D**), Cu (**E** and **F**), and Mn (**G** and **H**) for Columns 1 and 2. Unshaded region indicates Phase 1, grey shaded region indicates Phase 2, blue shaded region indicates Phase 3. Black dashed lines indicate input solution concentrations in each phase of the experiment. Note different scales for different elements.

4. Discussion

The results of the current column experiment show high removal of metals with Zn concentrations reaching half the input concentration during Phases 1 and 2 (Fig. 6E and F). This indicates that large quantities of Zn were adsorbed by the sediment, even though the column packing consisted of only 15 % organic, wetland sediment. Other metals were also immobilized in Column 2, with Pb dropping below detection limits in Phases 1 and 2 (Fig. 6A and B). Because the organic sediment was not the majority of the column packing, higher attenuation efficiencies could likely be achieved in the sediment, as was observed by Harper et al. [31] at the Ore

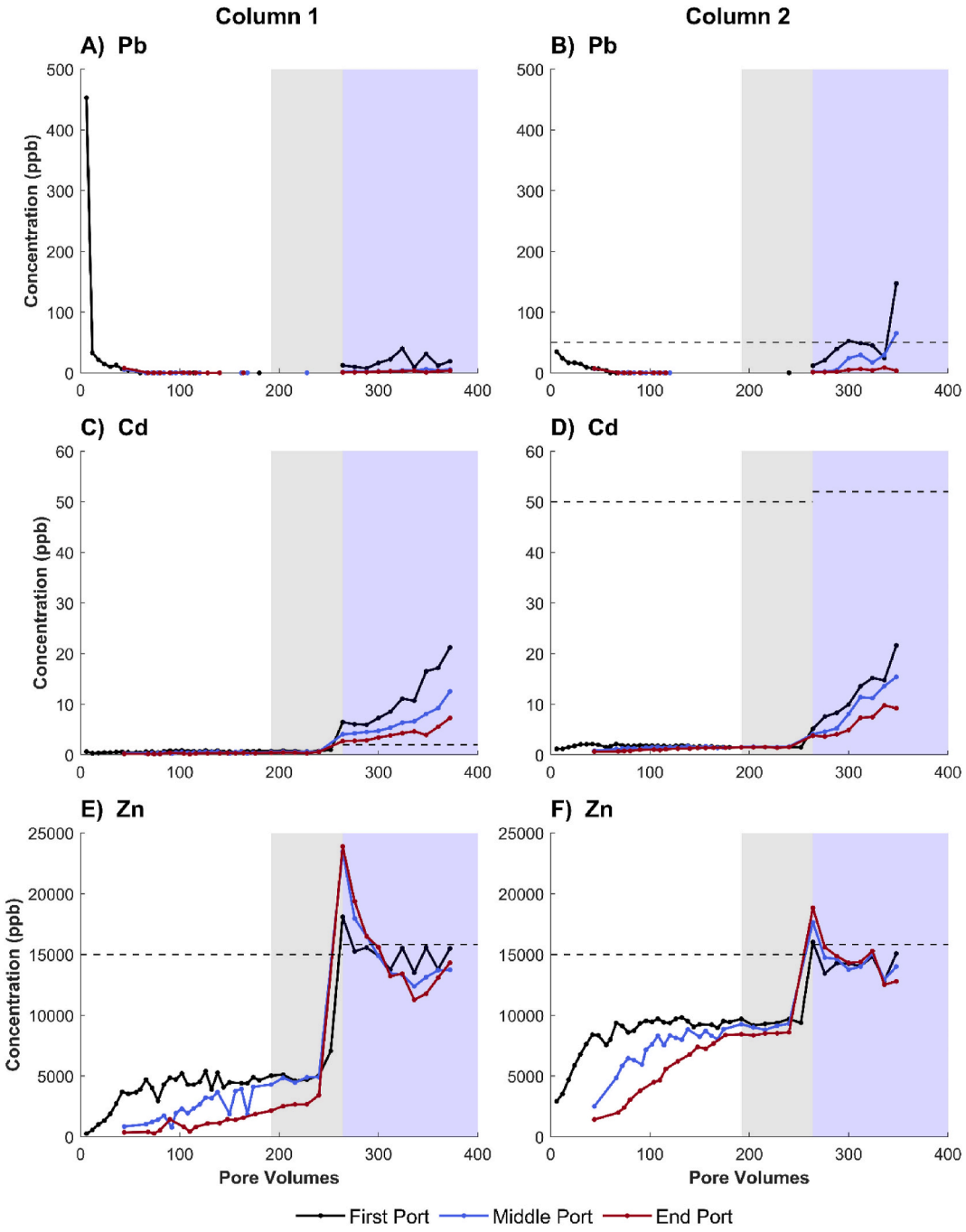

Fig. 6. Dissolved (<0.01 μm) metal concentrations for samples collected from sampling ports (indicated by line colours) for Pb (**A** and **B**), Cd (**C** and **D**), and Zn (**E** and **F**) from Columns 1 and 2. Unshaded region indicates Phase 1, grey region indicates Phase 2, blue region indicates Phase 3. Black dashed lines indicate input solution concentrations in each phase of the experiment. Note different scales for different elements. All metals plotted with 0.01 μm filtrate.

Chimney wetland. At the site, metal immobilization in the wetland sediment continues to occur even after approximately 100 years of drainage. Zinc concentrations in the sediment reach up to 9000 mg/kg [31] indicating high attenuation is possible in this sediment.

Similar metal removal results have also been obtained in other, relatively young, constructed wetlands used for the treatment of contaminated water. For example, Gandy et al. [43] showed treatment efficiencies of over 65 % for Zn could be achieved in a pilot scale short hydraulic residence time wetland constructed with compost, and Song et al. [44] showed that laboratory scale constructed wetlands could remove approximately 90 % of Pb and just over 70 % of Zn. The Zn concentration in the mine discharge (input

Table 5
Average percent of total metal concentration associated with colloidal sizes (between 0.01 μm and 10 μm) and in the dissolved phase (<0.01 μm) for Column 1. Percentages that were found to be negative values or greater than 100 %, which resulted from testing variation, sample heterogeneity and/or contamination of samples that went through more filter steps, were replaced with 0 or 100 (%), respectively. Averages were only calculated if greater than 3 samples were available for calculation. NC indicates values that were not calculated.

Colloid Class →		First Port		Middle Port		End port	
		Colloidal	Dissolved	Colloidal	Dissolved	Colloidal	Dissolved
Metal	Phase	>0.01 μm (%)	<0.01 μm (%)	>0.01 μm (%)	<0.01 μm (%)	>0.01 μm (%)	<0.01 μm (%)
Al	**1**	43.8	56.2	53.8	46.2	59.9	40.1
	2	64.3	35.7	54.6	45.4	52.8	47.2
	3	41.6	58.4	38.7	61.3	21.2	78.8
Mn	**1**	0	100	0	100	0	100
	2	0	100	0	100	0	100
	3	1.4	98.6	0	100	0	100
Fe	**1**	25.0	74.1	39.2	61.4	35.1	64.9
	2	NC	NC	NC	NC	NC	NC
	3	32.5	67.5	25.4	74.6	11.3	88.7
Cu	**1**	25.9	74.1	33.1	66.9	37.1	62.9
	2	19.9	75.2	22.5	76.9	25.4	74.6
	3	35.7	64.3	12.9	87.1	0	100
Zn	**1**	12.9	87.1	6.0	94.0	0	100
	2	11.0	89.0	7.3	92.7	8.4	91.6
	3	9.4	90.6	5.5	94.5	4.5	95.5
Cd	**1**	13.6	86.4	8.9	91.1	19.9	80.1
	2	15.0	85.0	0	100	0.6	99.4
	3	15.9	84.1	0	100	0	100

Table 6
Average percent of total metal concentration associated with colloidal sizes (between 0.01 μm and 10 μm) and in the dissolved phase (<0.01 μm) for Column 2. Percentages that were found to be negative values or greater than 100 %, which resulted from testing variation, sample heterogeneity and/or contamination of samples that went through more filter steps, were replaced with 0 or 100 (%), respectively. Averages were only calculated if greater than 3 samples were available for calculation. NC indicates values that were not calculated.

Colloid Class →		First Port		Middle Port		End port	
		Colloidal	Dissolved	Colloidal	Dissolved	Colloidal	Dissolved
Metal	Phase	>0.01 μm (%)	<0.01 μm (%)	>0.01 μm (%)	<0.01 μm (%)	>0.01 μm (%)	<0.01 μm (%)
Al	**1**	38.3	61.7	47.1	52.9	57.5	42.5
	2	42.9	57.1	28.4	71.6	49.1	50.9
	3	49.7	50.3	42.9	57.1	47.3	52.7
Mn	**1**	0	100	0	100	0	100
	2	0	100	0	100	0	100
	3	3.6	96.4	0.6	99.4	0.4	99.6
Fe	**1**	0	100	3.1	98.2	26.0	74.0
	2	NC	NC	NC	NC	NC	NC
	3	44.2	55.8	32.9	67.1	35.8	64.2
Ni	**1**	4.0	96.0	3.7	96.3	2.2	97.8
	2	2.8	97.2	1.8	98.2	2.2	97.8
	3	10.7	89.3	5.2	94.8	4.4	95.6
Cu	**1**	15.9	83.9	22.1	77.9	24.8	75.2
	2	21.1	78.9	0	100	2.1	97.9
	3	46.5	53.5	33.4	66.6	29.8	70.2
Zn	**1**	5.1	94.9	5.6	94.4	7.1	92.9
	2	0.8	99.2	0.1	99.9	3.0	97.0
	3	7.3	92.7	2.8	97.2	1.9	98.1
Cd	**1**	38.3	61.7	47.1	52.9	57.5	42.5
	2	42.9	57.1	28.4	71.6	49.1	50.9
	3	49.7	50.3	42.9	57.1	47.3	52.7

conditions) studied by both Gandy et al. [43] and Song et al. [44] was lower than those studied here, but flow rates in the wetland studied by Gandy et al. [43] were higher than in the current experiment (approximately 150 m/year compared to 100 m/year in the columns in Phase 1), which may have contributed to the different removal efficiency. When the flow rate was increased in Phase 2 of the current experiment, removal efficiency did not go down indicating that the differences in substrate between all of these studies likely impacted the removal efficiency more.

Comparisons between Columns 1 and 2 indicate that the mobility of Zn was impacted by competitive adsorption (Fig. 6E and F) [45]. When other metals were present (Column 2), the mobility of Zn was higher than when Zn was the only metal present in solution

Table 7
Percent of cation concentration associated with colloidal sizes (between 0.01 μm and 10 μm) and in the dissolved phase (<0.01 μm) for porewater samples from Columns 1 and 2.

Colloid Class →	Column 1		Column 2	
	Colloidal	Dissolved	Colloidal	Dissolved
Metal	>0.01 μm (%)	<0.01 μm (%)	>0.01 μm (%)	<0.01 μm (%)
Na	2.4	97.6	9.2	90.8
Mg	11.4	88.6	21.0	79.0
K	0.9	99.1	9.4	90.6
Ca	33.7	66.3	42.0	58.0
Al	84.5	15.5	91.1	8.9
Mn	27.1	72.9	36.2	63.8
Fe	63.5	36.5	88.2	11.8
Cu	76.2	23.8	62.2	37.8
Zn	47.1	52.9	89.8	10.2
Cd	60.1	39.9	52.0	48.0
Pb	47.1	52.9	71.6	28.4

indicating that other metals, including Pb and Cd were more likely to fill sorption sites than Zn. Interestingly, the effect of competitive adsorption was less pronounced in Phase 3 of this experiment when the more complete colloid suspension acted to facilitate metal mobility, in particular for Zn, when the input concentration was reached immediately at the start of Phase 3, regardless of metal solution composition.

High concentrations of colloids were not mobile, particularly during the first two phases of the experiment, even with continuous input of colloids (Fig. 3). The colloid concentration was higher than the input concentration in the first sample from the first port of Column 1, indicating particle release from the column packing, however this was not observed in Column 2 which had low colloid concentrations throughout Phases 1 and 2. Colloid concentrations decreased rapidly in both columns implying colloid collection within the column and a lack of particle transport. Because of minimal particle transport, the condition that particles must be mobile for colloid-facilitated transport to occur may not be met in the first two phases of the experiment. Conditions were more favorable for colloid-facilitated transport in Phase 3.

Little to no association was observed between the major cations and colloids in water samples, as evidenced by the low percentages of these elements that were found in the 0.01 μm–10 μm colloid size fractions (Tables 3 and 4). This is similar to the results of Chowdhury et al. [20] who determined that Na, Ca, and K were all transported in the aqueous phase in the porewater of unsaturated soils at an abandoned coal mine in Ohio, USA, even though colloid-facilitated transport was implicated for the transport of metals such as Zn, Mn, and Fe. It has also been shown by other researchers that Na and Ca act to alter colloid behaviour, rather than having the colloids act as a transport pathway for these elements. Grolimund and Borkovec [4] showed, experimentally, that a switch from a solution dominated by monovalent Na^+ ions to divalent Ca^{2+} ions, increased colloid immobilization on solid surfaces because of the strength of the interactions between the negatively charged solid surfaces and the positively charged ions. In the current experiment both the ionic strength and the concentration of divalent ions was lower in Column 1 than Column 2. It would therefore be anticipated that Column 1 would have higher overall colloid mobility as particles would be less likely to be collected on solid surfaces through physical-chemical collection [3]. This was observed in the first approximately 15 pore volumes where the colloid concentration was higher in Column 1 samples than in Column 2 (Fig. 3), however it was not the case for the remainder of the experiment with both columns having low colloid concentrations in samples and a colloid concentration increase in Phase 3 of roughly the same amount.

The low percentages of Mn, Zn, and Cd associated with colloids studied (between 0.01 μm and 10 μm) in water samples indicates that these metals were primarily transported in the dissolved phase and colloids did not have a substantial impact on their transport behaviour (Tables 5 and 6). These findings are similar to those of Baumann et al. [46] who determined that the majority of metals studied in landfill leachate and un-impacted groundwater were found in the dissolved phase (defined as less than 0.001 μm in their study) or associated with less mobile particles greater than 1 μm in size. Baumann et al. [46] also attributed the high percentage of metals found in the dissolved phase to low colloid concentrations at one of the landfill sites studied, a finding that could apply to the current experiment since colloid concentrations in water samples were generally low, particularly in Phases 1 and 2.

In Column 1, Al, Fe, and Cu had high concentrations in the first several water samples collected at sample ports, but the concentration quickly decreased (Fig. 5). Although Al and Fe were not included in the input solutions, release occurred over several pore volumes indicating an initial flushing from the system and then slower release over time. It was determined that the percent of Al, Fe, and Cu associated with the colloid-size fraction was high (up to 65 % Al, up to 45 % Fe, and up to 50 % Cu) in both columns (Tables 5 and 6). While these high associations with colloids were observed, concentrations of these metals were relatively low in water samples throughout the experiments (approximate maximum concentration of Al at 3000 ppb (decreasing trend), Fe at 550 ppb (decreasing trend), and Cu at 500 ppb) so the mobility of these metals was still quite low. It is possible that these elements were being observed in the structure of the particles (i.e., colloid structures contained Al or Fe), associated with the surface of particles (i.e., adsorbed), as well as in the dissolved phase (i.e., not associated with particles).

Since the degree of association between metals and colloids above 0.1 μm in porewater extracted from the column packing at the end of the experiment was high (Table 7), there is further support that larger, less mobile particles were aiding in the immobilization of metals in the current experiment, similar to what was determined by Baumann et al. [46]. Data from extracted porewater indicated

that high proportions of metals were found between 1 and 10 μm in Column 1, while high proportions of metals were found between 0.1 μm and 1 μm in Column 2. Because these colloids had limited mobility under water flow conditions and were only removed from column packing under centrifugal force, it is possible to conclude that these size fractions aided in the removal of metal contaminants from solution and added to the sorption capacity of the sediment.

The increase in trace metal concentration observed in Phase 3 indicates that some portion of the more complete colloid suspension used during this phase facilitated metal transport through the columns. It was determined that the colloid suspension added significant concentrations of the major cations to the input solution, but added only minor amounts of metals, so it can be concluded that the suspension was facilitating metal transport, not simply increasing the concentration being added to the system. This can be seen particularly for Cd which was not mobile prior to Phase 3 but began to increase in both columns with the change in colloid suspension. It is possible that the near-identical trend observed for the two columns, despite the different input concentrations, resulted from the liberation of cadmium in the column packing and the enhanced transport facilitated by the smaller particles present in the suspension.

Although in the current study particles smaller than 0.01 μm are categorized as being in the dissolved phase, the increase in metal concentrations and mobility in Phase 3, when the smallest colloids were included in the input, indicates that these small particles are facilitating transport. While the composition of the colloids in this study was not directly characterized, it is possible that they are humic in nature due to the organic composition of the sediment. Increased metal mobility caused by humic acid is consistent with other research which has shown that mineral colloids can be stabilized by organic matter [19,47]. However, it is also possible that organic substances were acting directly as metal carriers in the current experiment, consistent with research on constructed wetlands [11]. Though not specifically addressed in this study, additional experiments that characterize the relationship between dissolved and total organic carbon and metals would make it possible to determine if the colloids are organic in nature.

5. Conclusion

The impacts of colloids on the mobility of Zn and other metals were studied experimentally. Results indicate that Zn was mobile in the organic wetland sediment and mobility was enhanced when other metals were present in solution due to competitive adsorption. Metal mobility was low and metals were immobilized in the column in the first two phases of the experiment, but the more complete colloid suspension used in the third phase of the experiment resulted in enhanced metal mobility, indicating that small particles, potentially humic acids below 0.01 μm in size, were responsible for facilitating metal transport. While these small particles were mobile in the columns, larger particles were not, similar to the findings of other researchers; however, these small particles were not removed by filtration and were therefore considered part of the dissolved phase (defined as anything less than 0.01 μm in size). The results of this study provide evidence that colloid-facilitated metal transport can occur in wetland sediment, but that small particles that are often considered "dissolved" are the dominant size-fraction enhancing metal transport.

CRediT authorship contribution statement

Colleen O. Harper: Conceptualization, Formal analysis, Investigation, Methodology, Visualization, Writing – original draft, Writing – review & editing. **Richard T. Amos:** Conceptualization, Funding acquisition, Methodology, Supervision, Writing – review & editing.

Funding

This work was supported by: the Natural Sciences and Engineering Research Council of Canada (NSERC) Discovery Grant awarded to Dr. Richard Amos and an NSERC Alexander Graham Bell Canada Graduate Scholarship awarded to Colleen Harper; the Ontario Research Fund – Research Excellence Grant "Integrated Tools and Technologies for Environmentally Responsible Management of Metal-bearing Wastes" awarded to Dr. David Blowes and Dr. Carol Ptacek (University of Waterloo) by the Ontario Ministry of Research, Innovation, and Science; and Carleton University.

Declaration of competing interest

The authors declare the following financial interests/personal relationships which may be considered as potential competing interests: Colleen Harper reports financial support was provided by Natural Sciences and Engineering Research Council of Canada (NSERC). Richard Amos reports financial support was provided by Ontario Ministry of Research, Innovation, and Science. Richard Amos reports financial support was provided by Natural Sciences and Engineering Research Council of Canada (NSERC).

Acknowledgements

The authors would like to acknowledge Imogen Addis and Karl Wasslen for their technical assistance, and Dr. Tom Al and Dr. Julie Brown for their helpful comments on a draft of the manuscript. Garry Smith and John Archibald (Devon Geological Services) granted access to the field site. This manuscript greatly benefitted from the comments of anonymous reviewers.

Appendix A. Supplementary data

Supplementary data to this article can be found online at https://doi.org/10.1016/j.heliyon.2024.e41223.

References

[1] D.W. Blowes, C.J. Ptacek, J.L. Jambor, C.G. Weisener, D. Paktunc, W.D. Gould, D.B. Johnson, 11.5 - the geochemistry of acid mine drainage, in: H.D. Holland, K. K. Turekian (Eds.), Treatise on Geochemistry, second ed., Elsevier, Oxford, 2014, pp. 131–190, https://doi.org/10.1016/B978-0-08-095975-7.00905-0.

[2] R.T. Amos, D.W. Blowes, B.L. Bailey, D.C. Sego, L. Smith, A.I.M. Ritchie, Waste-rock hydrogeology and geochemistry, Appl. Geochem. 57 (2015) 140–156, https://doi.org/10.1016/j.apgeochem.2014.06.020.

[3] J.F. McCarthy, J.M. Zachara, Subsurface transport of contaminants, Environ. Sci. Technol. 23 (1989) 496–502, https://doi.org/10.1021/es00063a001.

[4] D. Grolimund, M. Borkovec, Colloid-facilitated transport of strongly sorbing contaminants in natural porous media: mathematical modeling and laboratory column experiments, Environ. Sci. Technol. 39 (2005) 6378–6386, https://doi.org/10.1021/es050207y.

[5] T. Kanti Sen, K.C. Khilar, Review on subsurface colloids and colloid-associated contaminant transport in saturated porous media, Adv. Colloid Interface Sci. 119 (2006) 71–96, https://doi.org/10.1016/j.cis.2005.09.001.

[6] J.N. Ryan, M. Elimelech, Colloid mobilization and transport in groundwater, Colloids Surf. A Physicochem. Eng. Asp. 107 (1996) 1–56, https://doi.org/10.1016/0927-7757(95)03384-X.

[7] J. Yang, M. Ge, Q. Jin, Z. Chen, Z. Guo, Co-transport of U(VI), humic acid and colloidal gibbsite in water-saturated porous media, Chemosphere 231 (2019) 405–414, https://doi.org/10.1016/j.chemosphere.2019.05.091.

[8] D. Deb, S. Chakma, Colloid and colloid-facilitated contaminant transport in subsurface ecosystem—a concise review, Int. J. Environ. Sci. Technol. 20 (2023) 6955–6988, https://doi.org/10.1007/s13762-022-04201-z.

[9] J.F. McCarthy, L.D. McKay, Colloid transport in the subsurface: past, present, and future challenges, Vadose Zone J. 3 (2004) 326–337, https://doi.org/10.2113/3.2.326.

[10] J. Won, X. Wirth, S.E. Burns, An experimental study of cotransport of heavy metals with kaolinite colloids, J. Hazard Mater. 373 (2019) 476–482, https://doi.org/10.1016/j.jhazmat.2019.03.110.

[11] X. Xu, G.L. Mills, Do constructed wetlands remove metals or increase metal bioavailability? J. Environ. Manag. 218 (2018) 245–255, https://doi.org/10.1016/j.jenvman.2018.04.014.

[12] X. Wei, D. Pan, Z. Xu, D. Xian, X. Li, Z. Tan, C. Liu, W. Wu, Colloidal stability and correlated migration of illite in the aquatic environment: the roles of pH, temperature, multiple cations and humic acid, Sci. Total Environ. 768 (2021) 144174, https://doi.org/10.1016/j.scitotenv.2020.144174.

[13] M. Kheirabadi, M.H. Niksokhan, B. Omidvar, Colloid-associated groundwater contaminant transport in homogeneous saturated porous media: mathematical and numerical modeling, Environ. Model. Assess. 22 (2017) 79–90, https://doi.org/10.1007/s10666-016-9518-2.

[14] D. Grolimund, K. Barmettler, M. Borkovec, Colloid facilitated transport in natural porous media: fundamental phenomena and modelling, in: F.H. Frimmel, F. Von Der Kammer, H.-C. Flemming (Eds.), Colloidal Transport in Porous Media, Springer, Berlin, Heidelberg, 2007, pp. 3–27, https://doi.org/10.1007/978-3-540-71339-5_1.

[15] M. Takala, P. Manninen, Sampling and analysis of groundwater colloids - a literature review, Posiva, https://inis.iaea.org/collection/NCLCollectionStore/_Public/43/061/43061163.pdf, 2006. (Accessed 4 January 2021).

[16] R. Kretzschmar, T. Schäfer, Metal retention and transport on colloidal particles in the environment, Elements 1 (2005) 205–210, https://doi.org/10.2113/gselements.1.4.205.

[17] Y. Jiang, L. Yu, H. Sun, X. Yin, C. Wang, S. Mathews, N. Wang, Transport of natural soil nanoparticles in saturated porous media: effects of pH and ionic strength, Chem. Speciat. Bioavailab. 29 (2017) 186–196, https://doi.org/10.1080/09542299.2017.1403293.

[18] Y. Kalmykova, S. Rauch, A.-M. Strömvall, G. Morrison, B. Stolpe, M. Hassellöv, Colloid-facilitated metal transport in peat filters, Water Environ. Res. 82 (2010) 506–511.

[19] J. Ma, H. Guo, L. Weng, Y. Li, M. Lei, Y. Chen, Distinct effect of humic acid on ferrihydrite colloid-facilitated transport of arsenic in saturated media at different pH, Chemosphere 212 (2018) 794–801, https://doi.org/10.1016/j.chemosphere.2018.08.131.

[20] M.A.R. Chowdhury, D.M. Singer, E. Herndon, Colloidal metal transport in soils developing on historic coal mine spoil, Appl. Geochem. 128 (2021) 104933, https://doi.org/10.1016/j.apgeochem.2021.104933.

[21] M.A.R. Chowdhury, D.M. Singer, Trace metal enrichment in the colloidal fraction in soils developing on abandoned mine spoils, Minerals 12 (2022) 1290, https://doi.org/10.3390/min12101290.

[22] L. Denaix, R.M. Semlali, F. Douay, Dissolved and colloidal transport of Cd, Pb, and Zn in a silt loam soil affected by atmospheric industrial deposition, Environ. Pollut. 114 (2001) 29–38, https://doi.org/10.1016/S0269-7491(00)00204-9.

[23] L. Pang, M. Close, A field study of nonequilibrium and facilitated transport of Cd in an alluvial gravel aquifer, Ground Water 37 (1999) 785–792, https://doi.org/10.1111/j.1745-6584.1999.tb01171.x.

[24] L.E. Schemel, B.A. Kimball, K.E. Bencala, Colloid formation and metal transport through two mixing zones affected by acid mine drainage near Silverton, Colorado, Appl. Geochem. 15 (2000) 1003–1018, https://doi.org/10.1016/S0883-2927(99)00104-3.

[25] E.F. da Silva, C. Patinha, P. Reis, E.C. Fonseca, J.X. Matos, J. Barrosinho, J.M.S. Oliveira, Interaction of acid mine drainage with waters and sediments at the Corona stream, Lousal mine (Iberian Pyrite Belt, Southern Portugal), Environ. Geol. 50 (2006) 1001–1013, https://doi.org/10.1007/s00254-006-0273-6.

[26] Y.T.J. Kwong, C.F. Roots, P. Roach, W. Kettley, Post-mine metal transport and attenuation in the Keno Hill mining district, central Yukon, Canada, Environ. Geol. 30 (1997) 98–107, https://doi.org/10.1007/s002540050137.

[27] B.J. McNeill, E. Pakostova, J.G. Bain, W.D. Gould, R.T. Amos, G.W. Wilson, C.J. Ptacek, D.W. Blowes, Microbial community structure within a weathered waste-rock pile overlain by a monolayer soil cover, Appl. Geochem. 114 (2020) 104531, https://doi.org/10.1016/j.apgeochem.2020.104531.

[28] C.D. Church, R.T. Wilkin, C.N. Alpers, R.O. Rye, R.B. McCleskey, Microbial sulfate reduction and metal attenuation in pH 4 acid mine water, Geochem. Trans. 8 (2007) 10, https://doi.org/10.1186/1467-4866-8-10.

[29] M. Ranville, D. Rough, A. Russell Flegal, Metal attenuation at the abandoned Spenceville copper mine, Appl. Geochem. 19 (2004) 803–815, https://doi.org/10.1016/j.apgeochem.2003.09.013.

[30] A. Hicks, Investigating Mineral Weathering and Metal Transport through Century-Old Ore Chimney Waste Rock, Carleton University, 2021. https://curve.carleton.ca/1db5f0a4-b0aa-4e7e-b1d0-7d913bade818. (Accessed 10 December 2021).

[31] C. Harper, C. Walsh, C. Fong, P.R. Gammon, R.T. Amos, Long-term zinc contamination and transport at the abandoned Ore Chimney mine, Can. Geotech. J. 58 (2021) 1495–1512, https://doi.org/10.1139/cgj-2020-0270.

[32] E.P. Dillon, Gold-Quartz-Arsenopyrite Vein Deposits Localized Near the Base of the Flinton Group, Kaladar and Barrie Townships, Southeastern Ontario, Ministry of Natural Resources, 1985. https://www.geologyontario.mndm.gov.on.ca/mndmfiles/pub/data/imaging/OFR5529/OFR5529.pdf. (Accessed 4 June 2021).

[33] J.M. Moore, R.L. Morton, Geology of the Marble Lake Area, Counties of Frontenac and Lennox and Addington, Ministry of Northern Development and Mines, Toronto, 1986. https://www.geologyontario.mndmf.gov.on.ca/mndmfiles/pub/data/imaging/R238/R238.pdf. (Accessed 3 June 2021).

[34] L. Harnois, J.M. Moore, Geochemistry and origin of the Ore Chimney formation, a transported paleoregolith in the grenville province of southeastern Ontario, Canada, Chem. Geol. 69 (1988) 267–289, https://doi.org/10.1016/0009-2541(88)90039-3.

[35] L. Harnois, J.M. Moore, Geochemistry and genesis of two unconformity-associated gold deposits at the base of the Flinton Group, Grenville Province, southeastern Ontario, Canada, Econ. Geol. 84 (1989) 676–693, https://doi.org/10.2113/gsecongeo.84.3.676.
[36] National air photo library, aerial photograph a4862-95 (photo_19341009_N44773W077158). https://www.eodms-sgdot.nrcan-rncan.gc.ca/index-en.html, 1934. (Accessed 15 February 2022).
[37] D.A. Irwin, The Long Lake Zinc Mine and the Ore Chimney Gold Mine, Southeastern Ontario: A Geophysical Exploration Guideline, Carleton University; Ottawa-Carleton Geoscience Centre, 1992. https://curve.carleton.ca/system/files/etd/31ac0733-fd76-4721-9cfc-701536bbb367/etd_pdf/9e487263613d87dcb94c56367c6fcd57/irwin-thelonglakezincmineandtheorechimneygoldmine.pdf. (Accessed 25 September 2018).
[38] S.B. Roy, D.A. Dzombak, Chemical factors influencing colloid-facilitated transport of contaminants in porous media, Environ. Sci. Technol. 31 (1997) 656–664, https://doi.org/10.1021/es9600643.
[39] J.R. Lead, W. Davison, J. Hamilton-Taylor, J. Buffle, Characterizing colloidal material in natural waters, Aquat. Geochem. 3 (1997) 213–232, https://doi.org/10.1023/A:1009695928585.
[40] R.E. Wolf, M. Adams, Multi-elemental Analysis of Aqueous Geochemical Samples by Quadrupole Inductively Coupled Plasma-Mass Spectrometry (ICP-MS), U.S. Geological Survey, 2015, https://doi.org/10.3133/ofr20151010.
[41] N. Merlin, V.A. Lima, L.M. Santos-Tonial, Instrumental and experimental conditions for the application of fourier transform infrared analysis on soil and humic acid samples, combined with chemometrics Tools and scanning electron microscopy, J. Braz. Chem. Soc. 26 (2015) 1920–1927, https://doi.org/10.5935/0103-5053.20150170.
[42] W.A. Price, Prediction Manual for Drainage Chemistry from Sulphidic Geological Materials, CANMET - Mining and Mineral Sciences Laboratories, British Columbia, Canada, 2009. http://mend-nedem.org/wp-content/uploads/1.20.1_PredictionManual.pdf. (Accessed 8 April 2019).
[43] C.J. Gandy, J.E. Davis, P.H.A. Orme, H.A.B. Potter, A.P. Jarvis, Metal removal mechanisms in a short hydraulic residence time subsurface flow compost wetland for mine drainage treatment, Ecol. Eng. 97 (2016) 179–185, https://doi.org/10.1016/j.ecoleng.2016.09.011.
[44] Y. Song, M. Fitch, J. Burken, L. Nass, S. Chilukiri, N. Gale, C. Ross, Lead and zinc removal by laboratory-scale constructed wetlands, Water Environ. Res. 73 (2001) 37–44, https://doi.org/10.2175/106143001X138660.
[45] C. Campillo-Cora, M. Conde-Cid, M. Arias-Estévez, D. Fernández-Calviño, F. Alonso-Vega, Specific adsorption of heavy metals in soils: individual and competitive experiments, Agronomy 10 (2020) 1113, https://doi.org/10.3390/agronomy10081113.
[46] T. Baumann, P. Fruhstorfer, T. Klein, R. Niessner, Colloid and heavy metal transport at landfill sites in direct contact with groundwater, Water Res. 40 (2006) 2776–2786, https://doi.org/10.1016/j.watres.2006.04.049.
[47] J. Yan, V. Lazouskaya, Y. Jin, Soil colloid release affected by dissolved organic matter and redox conditions, Vadose Zone J. 15 (2016), https://doi.org/10.2136/vzj2015.02.0026.